The 9th European Congress on Computational Methods in Applied Sciences and Engineering
ECCOMAS Congress 2024
3–7 June 2024, Lisboa, Portugal

PROJECTION BASED REDUCED ORDER MODEL OF ELASTO-ACOUSTIC VIBRATIONS COMPUTED WITH ISOGEOMETRIC ANALYSES

T. LANDI[1,2], C. HOAREAU[2], J.F.DEU[2], R.CITARELLA[1], and R.OHAYON[2]

[1] Department of Industrial Engineering, University of Salerno, Fisciano, SA, Italy
e-mail: tlandi@unisa.it
e-mail: rcitarella@unisa.it

[2] Structural Mechanics and Coupled Systems Laboratory, Conservatoire National Des Arts e Metiers, Paris, France
email: christophe.hoareau@lecnam.it
email: jean-francois.deu@lecnam.net
email: roger.ohayon@lecnam.net

Key words: Finite Element Method, Isogeometric Analysis, Modal Analysis, Projection of Modal Basis (PROMs)

Summary. This paper demonstrates the advantages of Isogeometric Analysis (IGA) over the Finite Element Method (FEM). The study applies IGA to a vibro-acoustic problem, comparing the results with those obtained using an analytical approach and FEM. Specifically, the problem involves a cylindrical cavity surrounded by an external structure. The analysis is carried out in three stages: solving the structural problem, addressing the acoustic problem, and finally tackling the combined vibro-acoustic problem. The comparison highlights the benefits of IGA over traditional Finite Element Analysis.

1 INTRODUCTION

The study of vibro-acoustic problems holds fundamental importance in various sectors, such as automotive [1] and aerospace [2] fields. Structures exhibit varying behaviors under the influence of surrounding fluids, necessitating coupled analysis [3]. Complex computational techniques such as the Finite Element Method (FEM), Boundary Element Method (BEM), and Fast Multipole Method (FMM) are employed for the analysis of these problems.

FEM analysis is widely used in industry due to its reliability and effectiveness. The latter method involves an initial design phase followed by a meshing phase to divide the structure into numerous small elements or volumes. The meshing phase can be particularly time-consuming for complex geometries [4]. Additionally, the size of the mesh influences the solution due to the geometry approximation it provides.

Challenges encountered in FEM have spurred the development of Isogeometric Analysis (IGA) [4], which integrates the functions used for describing geometry also for the approximation of the state variables such as pressure, displacement, and temperature. In Computer-Aided Design (CAD), NURBS (Non-Uniform Rational B-Splines) are commonly used to describe curves.

NURBS have advantageous properties for tackling complex problems compared to the Lagrange functions, typically used in FEM. These properties include always positive bases and higher continuity, leading to smoother functions [4, 5].

Despite being relatively recent, IGA has already found application in various engineering fields such as structural mechanics [6]. Hughes et al. [7] noted that as the interpolation polynomial order increases, NURBS remain stable, whereas Lagrange functions tend to diverge. This stability makes NURBS well-suited for polynomial degree refinement.

Li et al. [8] demonstrated that using smoother shape functions in coupled fluid-structural problems leads to more accurate solutions compared to Lagrange functions.

Based on a review of literature, IGA analysis appears promising for studying coupled fluid-structural problems.

This work aims to investigate the vibro-acoustic problem using the Isogeometric Approach. The paper will show some examples comparing IGA and FEM with an analytical solution [9], and The Projection of Modal Basis (PROMs) will be used to reduce the computational time for calculating the natural frequencies and the modal shapes.

2 Numerical Examples

This chapter presents numerical examples obtained from the study and it is divided into three sections: the first section addresses the structural problem, the second focuses on the acoustic problem, and the third covers the vibro-acoustic problem. In each section, the results in terms of natural frequencies and modal shapes obtained from an analytical solution [9], are compared with those obtained using FEM and IGA methods.

2.1 Structural problem

The structure under investigation is the one shown in [9]. It is an hollow cylinder (Figure 1), the dimensions and material characteristics of which are given in Table 1.

Table 1: Structural charateristics

$\rho_s \left[\frac{kg}{m^3}\right]$	Young Modulus[Pa]	Poisson[-]	External Radius[m]	Thickness[m]	Length[m]
2700	$7{\cdot}E^{10}$	0.3	1	0.05	3

Figure 1: Structural geometry

The boundary conditions for the structure specify that only the displacement along the axis of the cylinder is free at both the top and bottom ends, indicating that it is a simply supported cylinder.
To ensure consistency of results, the FEM and IGA problems are set to similar conditions by refining the meshes to achieve approximately the same number of degrees of freedom (DOFs), while maintaining a conservative approach with $DOFs_{FEM} > DOFs_{IGA}$. The same polynomial interpolation degree (p=2) is used for both configurations. The FEM and IGA meshes are shown in Figure 2.

(a) Structural FEM mesh

(b) Structural IGA mesh

Figure 2: FEM and IGA Structural Meshes

From Figure 2, it is evident that the two meshes are not identical. However, despite this difference, the degrees of freedom (DOFs) for FEM are 49920, while those for IGA are 49136, ensuring that $DOFs_{FEM} > DOFs_{IGA}$. The discrepancy in the meshes arises because the refinement strategies for FEM and IGA, although based on the same principles, do not yield the same number of elements [5]. Importantly, this difference does not lead to an increase in computational time, as the matrix assembly time is significantly less compared to the time required to solve the linear system, which computes the eigenvalues and eigenvectors of the system.
The linear system that needs to be solved to obtain the eigenvalues and eigenvectors of the system is:

$$\left(\mathbf{K} - \omega_s^2 \mathbf{M}\right)(U) = 0 \tag{1}$$

Where:
$\mathbf{K}$ = Structural stiffness matrix;
$\mathbf{M}$ = Structural mass matrix;
U = Structural unknown displacement amplitude;
ω_s = Structural circular natural frequency;

In Table 2, the first 10 frequencies obtained through the analytical solution [9], the FEM analysis, and IGA are shown. Additionally, the wavenumber of each mode is included (m = axial wavenumber; n = circumferential wavenumber). In Figure 3 the first three modal shapes, obtained from IGA, are also shown.

Table 2: First 10 structural frequencies and related wave-numbers computed with the analytical solution, FEM and IGA

m	n	Analytical solution[Hz]	FEM[Hz]	IGA[Hz]
1	3	1.357×10^2	1.357×10^2	1.357×10^2
1	2	1.584×10^2	1.584×10^2	1.584×10^2
1	4	2.042×10^2	2.043×10^2	2.042×10^2
2	4	2.880×10^2	2.880×10^2	2.880×10^2
2	3	2.889×10^2	2.889×10^2	2.889×10^2
1	5	3.140×10^2	3.143×10^2	3.141×10^2
1	1	3.151×10^2	3.151×10^2	3.151×10^2
2	5	3.683×10^2	3.685×10^2	3.684×10^2
2	2	3.987×10^2	3.986×10^2	3.987×10^2
3	4	4.231×10^2	4.233×10^2	4.231×10^2

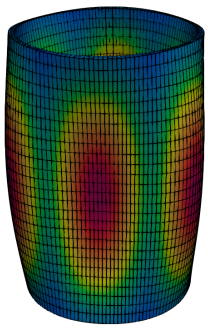

(a) Modal shape at 1.357×10^2 Hz

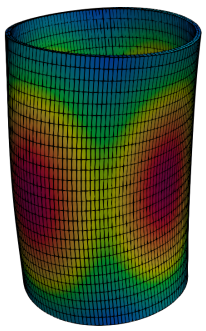

(b) Modal shape at 1.584×10^2 Hz

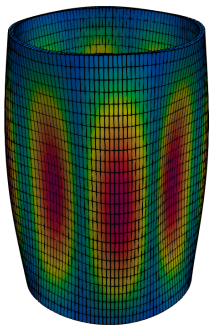

(c) Modal shape at 2.042×10^2 Hz

Figure 3: First three modal shapes computed with IGA

To better figure out the obtained results, it is useful to plot the percentage error of the FEM

and IGA frequencies compared to the reference analytical frequencies. The percentage error can be defined as in the Equation 2 and its trend is shown in Figure 4

$$\text{Error } [\%] = \left| \left(\frac{f_{\text{IGA/FEM}}}{f_{\text{ANALYTICAL}}} - 1 \right) \times 100 \right| \tag{2}$$

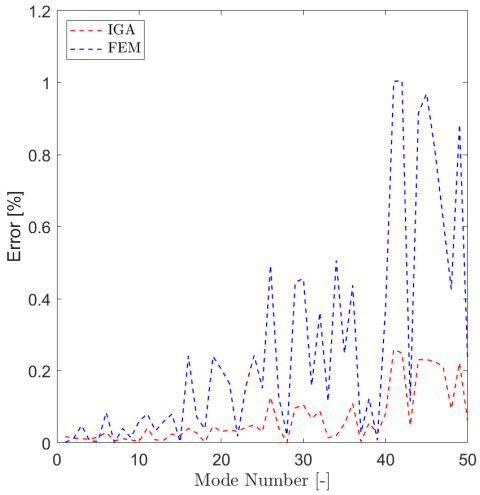

Figure 4: Error between the structural frequencies obtained from FEM/IGA and the analytical solution

As can be seen from Figure 4, although the FEM method has a low error (the maximum is around 1.1%), the Isogeometric Approach has a lower error, which proves its higher efficiency over FEM.

Additionally, a convergence analysis was conducted for the structural modes, evaluating the frequency obtained by increasing the degrees of freedom of the system. The convergence analysis for the first and third modes are shown in Figure 5.

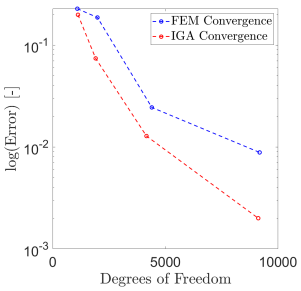

(a) Convergence analysis for the structural mode at 135.719 Hz

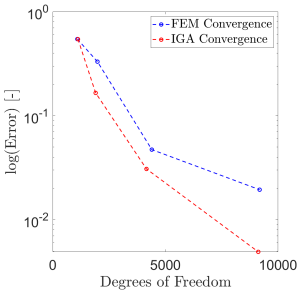

(b) Convergence analysis for the structural mode at 204.171 Hz

Figure 5: Convergence analysis for the structural modes at 135.719 Hz and 204.171 Hz

Figure 5 shows that the convergence of the IGA model is higher than that of the FEM one.

2.2 Acoustic problem

The procedure followed for the structural part is repeated for the acoustic side. The conditions imposed on the fluid cavity are those of rigid walls. The geometry is shown in Figure 6, material properties and dimensions are listed in Table 3. The FEM and IGA meshes are shown in Figure 7. Also in this case, the condition $DOFs_{FEM} > DOFs_{IGA}$ is satisfied ($DOFs_{FEM} = 16663$ and $DOFs_{IGA} = 15135$).

Table 3: Fluid Properties

$\rho_f \left[\frac{kg}{m^3}\right]$	$c_0 \left[\frac{m}{s}\right]$	Diameter[m]	Length[m]
1.2	340	0.95	3

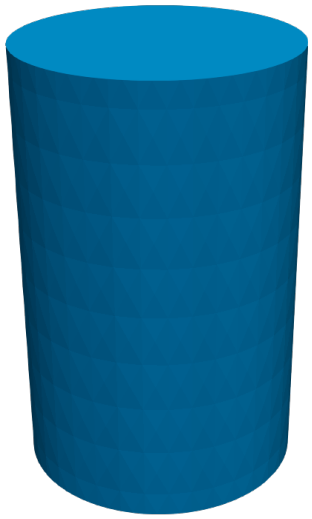

Figure 6: Fluid geometry

(a) Fluid FEM mesh

(b) Fluid IGA mesh

Figure 7: FEM and IGA Fluid Meshes

Solving the Equation 3, it is possible to get the eigenfrequencies and the eigenvectors for the acoustic problem.

$$\left(\mathbf{H} - \omega_f^2 \mathbf{Q}\right)(P) = 0 \tag{3}$$

Where:
$\mathbf{H}$ = Acoustic stiffness matrix;
$\mathbf{Q}$ = Acoustic mass matrix;
P = Acoustic unknown pressure amplitude;
ω_f = Acoustic circular natural frequency;

The obtained frequencies are shown in Table 4. m,n and k are the wave numbers in the axial, circumferential and radial direction, respectively.

Table 4: First 10 acoustic frequencies and related wave-numbers computed with analytical solution, FEM and IGA

m	n	k	Analytical solution[Hz]	FEM[Hz]	IGA[Hz]
1	0	0	56.667	56.667	56.667
0	1	1	104.875	104.875	104.875
2	0	0	113.333	113.352	113.338
1	1	0	119.205	119.206	119.205
2	1	0	154.413	154.426	154.416
3	0	0	170.00	170.134	170.036
0	2	1	173.972	173.972	173.972
1	2	0	182.968	182.968	182.968
3	1	0	199.747	199.861	199.777
2	2	0	207.631	207.641	207.633

The first three acoustic modal shapes, computed with IGA, are shown in Figure 8.

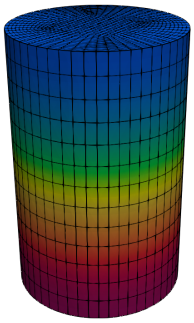

(a) Modal shape at 56.667 Hz

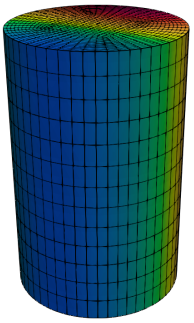

(b) Modal shape at 104.875 Hz

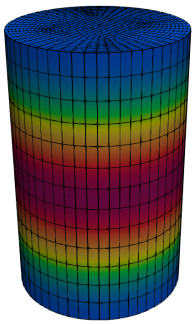

(c) Modal shape at 113.338 Hz

Figure 8: IGA acoustic modal shapes of the first three modes

Following the Equation 2, it is possible to plot the percentage error for the acoustic FEM/IGA mode frequencies respect to the analytical ones.

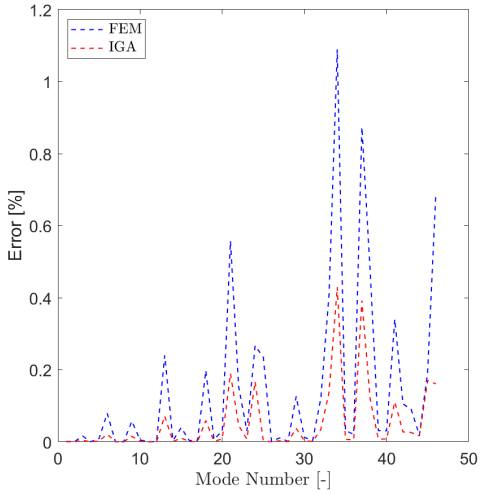

Figure 9: Error between the FEM and IGA acoustic modes respect to the analytical ones

As can be seen from Figure 9, although the FEM method has a low error (the maximum is around 1.1%), the Isogeometric Approach has a lower error, which proves its higher efficiency over FEM.

Additionally, a convergence analysis was conducted for the acoustic modes, evaluating the frequency obtained by increasing the degrees of freedom of the system. The convergence analysis for one mode is shown in Figure 10.

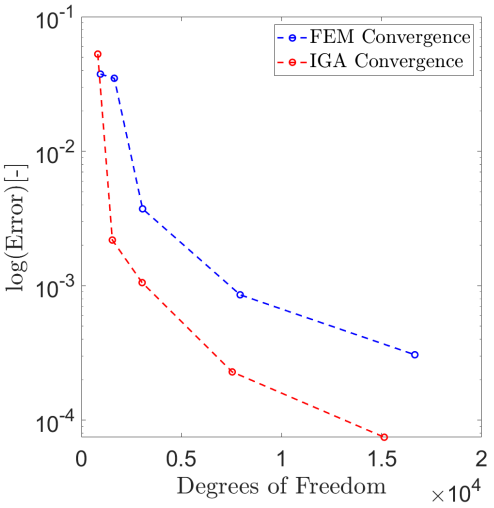

Figure 10: Convergence analysis for the acoustic mode at 293.540Hz

2.3 Vibro-acoustic problem

In this last section, the vibroacoustic problem is solved using FEM and IGA in combination with Projection of Modal Basis (PROMs) and compared with analytical results. In Figure 11, the

problem under investigation is depicted (cylinder filled with fluid). The material and geometric properties for both the structure and the fluid are as shown in Tables 1 and 3, respectively. The boundary conditions are also as stated earlier. Figure 12 shows the FEM and IGA meshes considered ($DOFs_{FEM} = 56281$ and $DOFs_{IGA} = 55021$).

Figure 11: Vibroacoustic Geometry

(a) Vibroacoustic FEM mesh

(b) Vibroacoustic IGA mesh

Figure 12: FEM and IGA Vibroacoustic Meshes

To solve the vibroacoustic problem, in order to find out the eigenvectors and the eigenvalues, it is necessary to solve the Equation 4.

$$\left(-\omega^2 \begin{bmatrix} \mathbf{M} & 0 \\ -\mathbf{C} & \mathbf{Q} \end{bmatrix} + \begin{bmatrix} \mathbf{K} & -\frac{1}{\rho_f} \cdot \mathbf{C}^T \\ 0 & \mathbf{H} \end{bmatrix}\right) \begin{pmatrix} U \\ P \end{pmatrix} = \begin{pmatrix} 0 \\ 0 \end{pmatrix} \tag{4}$$

Where $\mathbf{C}$ is the coupling matrix.
The resolution of this problem is computationally very demanding; therefore, the solution is obtained leveraging on the projection of modal basis.

First, the acoustic and structural problems are solved separately using Equations 1 and 3. Then, by using the uncoupled modes, it is possible to solve Equation 5.

$$\left(-\omega_c^2 \begin{bmatrix} \mathbf{M}_r & 0 \\ -\mathbf{C}_r & \mathbf{Q}_r \end{bmatrix} + \begin{bmatrix} \mathbf{K}_r & -\frac{1}{\rho_f} \cdot {\mathbf{C}_r}^T \\ 0 & \mathbf{H}_r \end{bmatrix} \right) \begin{pmatrix} \eta \\ \xi \end{pmatrix} = \begin{pmatrix} 0 \\ 0 \end{pmatrix} \tag{5}$$

Where:
$\mathbf{M}_r = {\boldsymbol{\phi_s}}^T \mathbf{M}\ \boldsymbol{\phi_s}$ = Reduced structural mass matrix;
$\mathbf{Q}_r = {\boldsymbol{\phi_f}}^T\ \mathbf{Q}\ \boldsymbol{\phi_f}$ = Reduced acoustic mass matrix;
$\mathbf{C}_r = {\boldsymbol{\phi_f}}^T \mathbf{C}\ \boldsymbol{\phi_s}$ = Reduced coupling matrix;
$\mathbf{K}_r = {\boldsymbol{\phi_s}}^T \mathbf{K}\ \boldsymbol{\phi_s}$ = Reduced structure stiffness matrix;
$\mathbf{H}_r = {\boldsymbol{\phi_f}}^T \mathbf{H}\ \boldsymbol{\phi_f}$ = Reduced acoustic stiffness matrix;
$\boldsymbol{\phi_s}$ = Structural modal basis;
$\boldsymbol{\phi_f}$ = Acoustic modal basis;
η = Structural modal displacement;
ξ = Acoustic modal pressure;
ω_c = Coupled circular natural frequency;

The reduced problem (Equation 5) can be solved more easily than the full problem (Equation 4). In fact, while in the full problem the matrix size is related to the number of degrees of freedom (DOFs) of the system, in the reduced problem it is related to the number of modes considered, with $\text{DOFs}_r \ll \text{DOFs}$.

In this case, given that the range of interest is [0-200]Hz, to calculate the coupled modes of the system using Equation 5, all acoustic and structural modes up to 450Hz are considered.

Table 5 shows the first 8 coupled frequencies calculated using the analytical solution [9], FEM, and IGA and their wave number.

Additionally, Figure 13 shows the modal shapes of the first two vibroacoustic modes computed with IGA.

Table 5: First 8 Vibroacoustic frequencies and related wave-numbers computed with Analytical solution, FEM and IGA

m	n	k	Analytical solution[Hz]	FEM[Hz]	IGA[Hz]
1	0	0	56.664	56.667	56.667
0	1	1	105.054	104.867	104.875
2	0	0	113.329	113.339	113.334
1	1	0	119.176	119.205	119.205
1	3	0	135.479	135.891	135.533
2	1	0	154.399	154.406	154.398
1	2	1	157.628	157.347	158.234
0	2	1	174.194	174.754	174.108

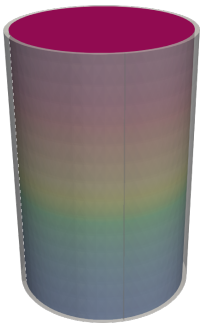

(a) Vibroacoustic mode at 56.667 Hz

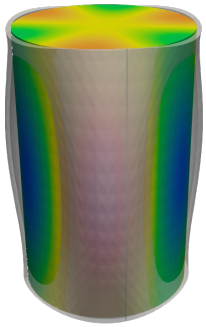

(b) Vibroacoustic mode at 135.533 Hz

Figure 13: Vibroacoustic modes at 56.667 Hz and 135.533 Hz

Figure 14 shows the error (Equation 2), which is useful for demonstrating the efficiency of IGA over FEM.

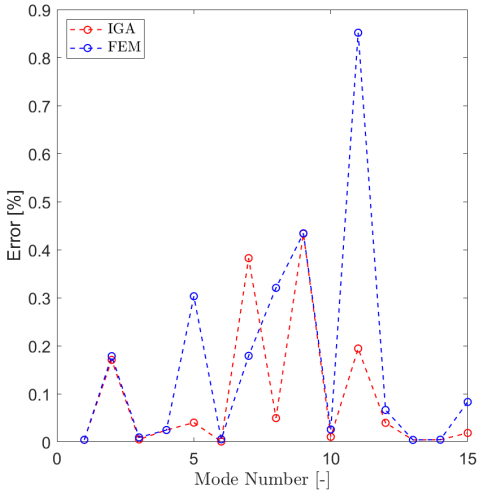

Figure 14: Error between the FEM and IGA Vibroacoustic Modes respect to the Analytical ones

As can be seen from Figure 14, although the FEM method has a low error (the maximum is around 0.85%), also in the vibroacoustic case, the Isogeometric Approach has a lower error, which proves its high efficiency over FEM.

3 CONCLUSIONS

In conclusion, this paper has demonstrated the advantages of the IGA approach over the FEM one by comparing the results with those of an analytical solution. As shown in Figures 4, 9, and 14, the frequency error obtained with IGA is more accurate than that obtained with FEM. The analyses were conducted under the same operating conditions, ensuring that both the IGA and FEM problems were evaluated under identical hypotheses.

Additionally, convergence analyses for both structural and acoustic parts also indicate superior performance of the IGA model compared to the FEM one. The IGA approach consistently demonstrates higher convergence rates, which highlights its effectiveness in solving complex problems with greater accuracy.

Moreover, further investigation is necessary to explore how the solution evolves with an increasing polynomial degree. As reported in [7], while the FEM method shows a divergence in the solution with higher polynomial degrees, the IGA method demonstrates improved behavior. This suggests that IGA not only provides better initial accuracy but also maintains stability and accuracy as the polynomial degree increases.

Overall, these findings underscore the potential of the IGA approach in various engineering applications, particularly where high accuracy and convergence are critical. Future research should continue to explore the capabilities of IGA, especially in more complex and varied problem settings, to fully harness its advantages over traditional FEM.

REFERENCES

[1] R. Citarella, T. Landi , L. Caivano, G. D'Errico, F. Raffa , M. Romano, E. Armentani, Structural and Vibro-Acoustics Optimization of a Car Body Rear Part. Appl. Sci. 2023, 13, 3552. https://doi.org/10.3390/app13063552

[2] R. Citarella ; L. Federico, Advances in Vibroacoustics and Aeroacustics of Aerospace and Automotive Systems. Appl. Sci. 2018, 8, 366. https://doi.org/10.3390/app8030366

[3] R., Ohayon ; C., Soize, "Contents," in Advanced Computational Vibroacoustics: Reduced-Order Models and Uncertainty Quantification, Cambridge: Cambridge University Press, 2014, pp. v–viii

[4] J.A. Cottrell,T.J. Hughes, Y. Bazilevs, Isogeometric Analysis: Toward Integration of CAD and FEA; John Wiley and Sons: Hoboken, NJ, USA, 2009, DOI:10.1002/9780470749081

[5] L. Piegl , W. Tiller, The NURBS Book, Springer-Verlag, New York, NY, USA, 1996

[6] T. Elguedj, Y. Bazilevs, V.M. Calo, T.J.R. Hughes, F-bar projection method for finite deformation elasticity and plasticity using NURBS based isogeometric analysis, Int J Mater Form 1 (2008) 1091–1094. https://doi.org/10.1007/s12289-008-0209-7.v

[7] T.J.R. Hughes, A. Reali, G. Sangalli, Duality and unified analysis of discrete approximations in structural dynamics and wave propagation: Comparison of p-method finite elements with k-method NURBS, Computer Methods in Applied Mechanics and Engineering 197 (2008) 4104–4124. https://doi.org/10.1016/j.cma.2008.04.006.

[8] W. Li, Y. Chai, M. Lei, G.R. Liu, Analysis of coupled structural-acoustic problems based on the smoothed finite element method (S-FEM), Engineering Analysis with Boundary Elements 42 (2014) 84–91. https://doi.org/10.1016/j.enganabound.2013.08.009.

[9] W. Larbi, J.-F. Deü, A 3D state-space solution for free-vibration analysis of a radially polarized laminated piezoelectric cylinder filled with fluid, Journal of Sound and Vibration 330 (2011) 162–181. https://doi.org/10.1016/j.jsv.2010.08.004.